

Towards Safe Reinforcement Learning Using NMPC and Policy Gradients: Part II - Deterministic Case

Sébastien Gros, Mario Zanon

Abstract—In this paper, we present a methodology to deploy the deterministic policy gradient method, using actor-critic techniques, when the optimal policy is approximated using a parametric optimization problem, where safety is enforced via hard constraints. For continuous input space, imposing safety restrictions on the exploration needed to deploying the deterministic policy gradient method poses some technical difficulties, which we address here. We will investigate in particular policy approximations based on robust Nonlinear Model Predictive Control (NMPC), where safety can be treated explicitly. For the sake of brevity, we will detail the construction of the safe scheme in the robust linear MPC context only. The extension to the nonlinear case is possible but more complex. We will additionally present a technique to maintain the system safety throughout the learning process in the context of robust linear MPC. This paper has a companion paper treating the stochastic policy gradient case.

Index Terms—Safe Reinforcement Learning, robust Model Predictive Control, stochastic policy gradient, interior-point method.

I. INTRODUCTION

Reinforcement Learning (RL) is a powerful tool for tackling Markov Decision Processes (MDP) without depending on a detailed model of the probability distributions underlying the state transitions. Indeed, most RL methods rely purely on observed state transitions, and realizations of the stage cost $L(\mathbf{s}, \mathbf{a}) \in \mathbb{R}$ assigning a performance to each state-input pair \mathbf{s}, \mathbf{a} (the inputs are often labelled actions in the RL community). RL methods seek to increase the closed-loop performance of the control policy deployed on the MDP as observations are collected. RL has drawn an increasingly large attention thanks to its accomplishments, such as, e.g., making it possible for robots to learn to walk or fly without supervision [19], [1].

Most RL methods are based on learning the optimal control policy for the real system either directly, or indirectly. Indirect methods typically rely on learning a good approximation of the optimal action-value function underlying the MDP. The optimal policy is then indirectly obtained as the minimizer of the value-function approximation over the inputs \mathbf{a} . Direct RL methods, based on policy gradients, seek to adjust the parameters θ of a given policy π_θ such that it yields the best closed-loop performance when deployed on the real system. An attractive advantage of direct RL methods over indirect ones is that they are based on formal necessary conditions of optimality for the closed-loop performance of π_θ , and there-

fore asymptotically (for a large enough data set) guarantee the (possibly local) optimality of the parameters θ [18], [17].

RL methods often rely on Deep Neural Networks (DNN) to carry the policy approximation π_θ . While effective in practice, control policies based on DNNs provide limited opportunities for formal verifications of the resulting closed-loop behavior, and for imposing hard constraints on the evolution of the state of the real system. The development of safe RL methods, which aims at tackling this issue, is currently an open field or research [12].

In this paper, we investigate the use of constrained parametric optimization problems to carry the policy approximation. The aim is to impose safety by means of hard constraints in the optimization problem. Most RL methods require exploration, i.e., the inputs applied to the real system must differ from the policy π_θ in order to identify changes in the policy parameters θ that can yield a higher closed-loop performance. Exploration is typically performed via stochastic disturbances of the policy. We will show in this paper that the presence of hard constraints distorts the statistics of the exploration, and that some corrections must in theory be introduced in the classic tools underlying the deterministic policy gradient method to account for this distortion. We propose computationally efficient tools to implement these corrections, based on parametric Nonlinear Programming techniques, and interior-point methods.

Robust Nonlinear Model Predictive Control (NMPC) is arguably an ideal candidate for forming the constrained optimization problem supporting the policy approximation. Robust NMPC techniques provide safety guarantees on the closed-loop behavior of the system by explicitly accounting for the presence of (possibly stochastic) disturbances and model inaccuracies. A rich theoretical framework is available on the topic [14]. The policy parameters θ will then appear as parameters in the NMPC model(s), cost function and constraints. Updates in the policy parameters θ will then be driven by the deterministic policy gradient method to increase the NMPC closed-loop performance, and constrained by the requirement that the NMPC model inaccuracies must be adequately accounted for in forming the robust NMPC scheme. For the sake of brevity and simplicity, we will detail these questions in the specific linear MPC case. The extension to the nonlinear case is arguably possible, but more complex.

This paper has a companion paper [10] treating the same problem in the context of the stochastic policy gradient approach. The two papers share the same background material, and some similar techniques. However, the theory allowing the deployment of the two policy gradient techniques is intrinsically different.

The paper is structured as follows. Section II provides

Sébastien Gros is with the Department of Cybernetic, NTNU, Norway.

Mario Zanon is with the IMT School for Advanced Studies Lucca, Lucca 55100, Italy.

some background material. Section III details the safe policy approximation we propose to use. Section IV establishes the basic properties that a safe exploration must fulfil in order to be able to build a correct policy gradient estimation with standard RL tools. Section V presents an optimization-based approach to generate an exploration satisfying these properties. Section VI discusses a technique to enforce safety in the RL-based learning process in the context of robust MPC. Section VII proposes an example of simulation using the principles developed in this paper.

II. BACKGROUND ON MARKOV DECISION PROCESSES

This section provides background material on Markov Decision Processes (MDP), and on their restriction to a safe set. We also provide a brief introduction to the deterministic policy gradient method.

A. Markov Decision Processes

In the following, we will consider that the dynamics of the real system are described as a Markov Process (MP), with state transitions having the underlying conditional probability density:

$$\mathbb{P}[\mathbf{s}_+ | \mathbf{s}, \mathbf{a}] \quad (1)$$

denoting the probability density of the state transition $\mathbf{s}, \mathbf{a} \rightarrow \mathbf{s}_+$. We will furthermore consider deterministic policies:

$$\mathbf{a} = \boldsymbol{\pi}(\mathbf{s}) \quad (2)$$

associating an input (a.k.a. action) $\mathbf{a} \in \mathbb{R}^{n_a}$ to any feasible state $\mathbf{s} \in \mathbb{R}^{n_s}$. In the following, it will be additionally useful to introduce the concept of stochastic policy

$$\pi[\mathbf{a} | \mathbf{s}] : \mathbb{R}^{n_a} \times \mathbb{R}^{n_s} \rightarrow \mathbb{R}_+ \quad (3)$$

denoting the probability density of selecting a given input \mathbf{a} for a given state \mathbf{s} . It is useful to observe that any deterministic policy (2) can be defined as a stochastic policy using:

$$\pi[\mathbf{a} | \mathbf{s}] = \delta(\mathbf{a} - \boldsymbol{\pi}(\mathbf{s})) \quad (4)$$

where δ is the Dirac function. All the definitions below then readily apply to both (3) and (2) by using (4). Let us consider the distribution of the MP resulting from the state transition (1) and policy (3):

$$\mathbb{P}[\mathbf{s}_k | \pi] = \int \prod_{i=0}^{k-1} \mathbb{P}[\mathbf{s}_{i+1} | \mathbf{s}_i, \mathbf{a}] \mathbb{P}[\mathbf{s}_0] \pi[\mathbf{a}_i | \mathbf{s}_i] \quad (5)$$

$$d\mathbf{s}_0, \dots, \mathbf{s}_{k-1} d\mathbf{a}_0, \dots, \mathbf{a}_{k-1}$$

where $\mathbb{P}[\mathbf{s}_0]$ denotes the probability distribution of the initial conditions \mathbf{s}_0 of the MP. We can then define the discounted expected value of the MP distribution under policy π , labelled $\mathbb{E}_\pi[\cdot]$, which reads as:

$$\mathbb{E}_\pi[\zeta] := \sum_{k=0}^{\infty} \int \gamma^k \zeta(\mathbf{s}_k, \mathbf{a}_k) \mathbb{P}[\mathbf{s}_k | \pi] \pi[\mathbf{a}_k | \mathbf{s}_k] d\mathbf{s}_k d\mathbf{a}_k \quad (6)$$

for any function ζ . In the following we will assume the local stability of the MP under the selected policies. More specifically, we assume that π is such that:

$$\lim_{\tilde{\pi} \rightarrow \pi} \mathbb{E}_{\tilde{\pi}}[\zeta] = \mathbb{E}_\pi[\zeta], \quad (7)$$

for any function ζ such that both sides of the equality are finite. Assumption (7) is underlying standard RL algorithms, though it is often left implicit, and allows us to draw equivalences between a policy and disturbances of that policy, which is required in the context of policy gradient methods. It can be construed as a local regularity assumption on $\mathbb{E}_\pi[\cdot]$ that, e.g., holds if the system dynamics in closed-loop with policy π are stable.

For a given stage cost function $L(\mathbf{s}, \mathbf{a})$ and a discount factor $\gamma \in [0, 1]$, the performance of a policy π is given by the discounted cost:

$$J(\pi) = \mathbb{E}_\pi[L] \quad (8)$$

The state transition (1), stage cost L and discount factor γ define a Markov Decision Process, with an underlying optimal policy given by:

$$\pi_\star = \arg \min_{\pi} J(\pi) \quad (9)$$

It is useful to underline here that, while (9) may have several (global) solutions, any fully observable MDP admits a deterministic policy π_\star among its solutions.

The (scalar) value function and action-value functions associated to a given policy π are given by [4], [6], [3]:

$$Q_\pi(\mathbf{s}, \mathbf{a}) = L(\mathbf{s}, \mathbf{a}) + \gamma \mathbb{E}[V_\pi(\mathbf{s}_+) | \mathbf{s}, \mathbf{a}], \quad (10a)$$

$$V_\pi(\mathbf{s}) = \mathbb{E}_{\mathbf{a} \sim \pi[\cdot | \mathbf{x}]}[Q_\pi(\mathbf{s}, \mathbf{a})], \quad (10b)$$

where the expected value in (10a) is taken over state transitions (1). The advantage function is then defined as:

$$A_\pi(\mathbf{s}, \mathbf{a}) = Q_\pi(\mathbf{s}, \mathbf{a}) - V_\pi(\mathbf{s}) \quad (11)$$

and provides the value of using input \mathbf{a} in a given state \mathbf{s} compared to using the policy π . Furthermore

$$A_{\pi_\star}(\mathbf{s}, \mathbf{a}) \geq 0, \quad \forall \mathbf{s}, \mathbf{a} \quad (12)$$

holds at the deterministic optimal policy π_\star .

B. Policy approximation and Deterministic policy gradient

In most cases, the optimal policy π_\star cannot be computed. It is then useful to consider approximations π_θ of the optimal policy, carried by a (possibly large) set of parameters θ . The optimal parameters θ_\star are then given by:

$$\theta_\star = \arg \min_{\theta} J(\pi_\theta) \quad (13)$$

The gradient associated to the minimization problem (13) is referred to as the *deterministic policy gradient* and is given by [17]:

$$\nabla_{\theta} J(\pi_\theta) = \mathbb{E}_{\pi_\theta}[\nabla_{\theta} \pi_\theta \nabla_{\mathbf{a}} A_{\pi_\theta}], \quad (14)$$

where $\nabla_{\mathbf{a}} A_{\pi_\theta}$ is the gradient of the advantage function (11). Reinforcement Learning algorithms based on the deterministic

policy gradient are forming estimations of (14) using observed state transitions. The gradient of the advantage function $\nabla_{\mathbf{a}} A_{\pi_{\theta}}$ in (14) is also estimated from the data.

One can observe that for any deterministic policy π_{θ} , the advantage function satisfies

$$A_{\pi_{\theta}}(\mathbf{s}, \pi_{\theta}(\mathbf{s})) = 0, \quad \forall \mathbf{s}, \quad (15)$$

hence in order to build estimations of the gradient $\nabla_{\mathbf{u}} A_{\pi_{\theta}}$, one needs to select inputs \mathbf{a} that depart from the deterministic policy π_{θ} , so as to be able to observe variations of $A_{\pi_{\theta}}$, see (12), and estimate its gradient. Selecting inputs $\mathbf{a} \neq \pi_{\theta}(\mathbf{s})$ in order to build the gradient $\nabla_{\mathbf{u}} A_{\pi_{\theta}}$ is referred to as *exploration*.

C. Safe set

In the following, we will assume the existence of a (possibly) state-dependent *safe set* labelled $\mathbb{S}(\mathbf{s}) \subseteq \mathbb{R}^{n_{\mathbf{a}}}$, subset of the input space. See [20], [10] for similar discussions. The notion of safe set will be used here in the sense that any input selected such that $\mathbf{a} \in \mathbb{S}(\mathbf{s})$ yields safe trajectories with a unitary probability. The construction of the safe set is not the object of this paper. However, we can nonetheless propose some pointer to how such a set is constructed in practice.

Let us consider the constraints $\mathbf{h}_{\mathbf{s}}(\mathbf{s}, \mathbf{a}) \leq 0$ describing the subset of the state-input space deemed feasible and safe. Constraints \mathbf{h} can include pure state constraints, describing the safe states, pure input constraints, typically describing actuators limitations, and mixed constraints, where the states and inputs are mixed. For the sake of simplicity, we will assume in the following that $\mathbf{h}_{\mathbf{s}}$ is convex.

A common approach to build practical or inner approximations of the safe set $\mathbb{S}(\mathbf{s})$ is via verifying the safety of an input \mathbf{a} explicitly over a finite horizon via predictive control techniques. This verification is based on forming the support of the Markov Process distribution over time, starting from a given state-input pair \mathbf{s}, \mathbf{a} . Consider the set $\mathbf{X}_{+}(\mathbf{s}, \mathbf{a})$, support of the state transition (1),

$$\mathbf{X}_{+}(\mathbf{s}, \mathbf{a}) = \{ \mathbf{s}_{+} \mid \mathbb{P}[\mathbf{s}_{+} \mid \mathbf{s}, \mathbf{a}] > 0 \} \quad (16)$$

Labelling $\mathbf{X}_k(\mathbf{s}, \mathbf{a}, \pi^{\mathbf{s}})$ the support of the state of the Markov Process at time k , starting from \mathbf{s}, \mathbf{a} and evolving under policy $\pi^{\mathbf{s}}$, the set \mathbf{X}_k is then given by the recursion:

$$\mathbf{X}_k(\mathbf{s}, \mathbf{a}, \pi^{\mathbf{s}}) = \mathbf{X}_{+}(\mathbf{X}_{k-1}, \pi^{\mathbf{s}}(\mathbf{X}_{k-1})), \quad (17)$$

with the boundary condition $\mathbf{X}_1 = \mathbf{X}_{+}(\mathbf{s}, \mathbf{a})$. An input \mathbf{a} is in the safe set $\mathbb{S}(\mathbf{s})$ if $\mathbf{h}_{\mathbf{s}}(\mathbf{s}, \mathbf{a}) \leq 0$ and if there exist a policy $\pi^{\mathbf{s}}$ such that

$$\mathbf{h}_{\mathbf{s}}(\mathbf{s}_k, \pi^{\mathbf{s}}(\mathbf{s}_k)) \leq 0, \quad \forall \mathbf{s}_k \in \mathbf{X}_k(\mathbf{s}, \mathbf{a}, \pi^{\mathbf{s}}), \quad (18)$$

for all $k \geq 1$. This verification is typically performed in practice via scenario trees, tube-based approaches, or direct approximations of the set \mathbf{X}_k via e.g. ellipsoids or polytopes [14].

In that context, policy $\pi^{\mathbf{s}}$ should ideally be identical to π_{θ} . However, for computational reasons, it is typically selected a priori to stabilize the system dynamics, and possibly optimized to minimize the size of the sets \mathbf{X}_k .

Due to the safety requirement, both the policy π_{θ} and the exploration performed by the RL algorithm will have to respect $\mathbf{a} \in \mathbb{S}(\mathbf{s})$, and can therefore not be chosen freely.

III. OPTIMIZATION-BASED SAFE POLICY

In this paper, we will consider parametrized deterministic policies π_{θ} based on parametric Nonlinear Programs (NLPs), and more specifically based on robust NMPC schemes. This approach is formally justified in [9]. More specifically, we will consider a policy approximation

$$\pi_{\theta} = \mathbf{u}_0^*(\mathbf{s}, \theta), \quad (19)$$

where $\mathbf{u}_0^*(\mathbf{s}, \theta)$ is the first $n_{\mathbf{a}}$ entries of $\mathbf{u}^*(\mathbf{s}, \theta)$ generated by the parametric NLP:

$$\mathbf{u}^*(\mathbf{s}, \theta) = \arg \min_{\mathbf{u}} \Phi(\mathbf{x}, \mathbf{u}, \theta) \quad (20a)$$

$$\text{s.t. } \mathbf{f}(\mathbf{x}, \mathbf{u}, \mathbf{s}, \theta) = 0, \quad (20b)$$

$$\mathbf{h}(\mathbf{x}, \mathbf{u}, \theta) \leq 0. \quad (20c)$$

We will then consider that the safety requirement $\pi_{\theta}(\mathbf{s}) \in \mathbb{S}(\mathbf{s})$ is imposed via the constraints (20b)-(20c). A special case of (20) is an optimization scheme in the form:

$$\mathbf{u}_0^*(\mathbf{s}, \theta) = \arg \min_{\mathbf{u}_0} \Phi(\mathbf{s}, \mathbf{u}_0, \theta) \quad (21a)$$

$$\text{s.t. } \mathbf{h}(\mathbf{s}, \mathbf{u}_0, \theta) \leq 0, \quad (21b)$$

where $\mathbf{h} \leq 0$ ought to ensure that $\pi_{\theta}(\mathbf{s}) = \mathbf{u}_0^*(\mathbf{s}, \theta) \in \mathbb{S}(\mathbf{s})$.

While most of the discussions in this paper will take place around the general formulation (20), a natural approach to formulate constraints (20b)-(20c) such that policy (19) is safe is to build (20) using robust (N)MPC techniques.

A. Policy approximation based on robust NMPC

The imposition of safety constraints can be treated via robust NMPC approaches. Robust NMPC can take different forms [14], all of which can be eventually cast in the form (20). One form of robust NMPC schemes is based on scenario trees [16], which take the form:

$$\mathbf{u}^*(\mathbf{s}, \theta) = \arg \min_{\mathbf{u}} \sum_{j=1}^{N_M} \left(V_j(\mathbf{x}_{j,N}, \theta) + \sum_{k=0}^{N-1} \ell_j(\mathbf{x}_{j,k}, \mathbf{u}_{j,k}, \theta) \right) \quad (22a)$$

$$\text{s.t. } \mathbf{x}_{j,k+1} = \mathbf{F}_j(\mathbf{x}_{j,k}, \mathbf{u}_{j,k}, \theta), \quad \mathbf{x}_{j,0} = \mathbf{s}, \quad (22b)$$

$$\mathbf{h}^{\mathbf{s}}(\mathbf{x}_{j,k}, \mathbf{u}_{j,k}, \theta) \leq 0, \quad (22c)$$

$$\mathbf{e}(\mathbf{x}_{j,N}, \theta) \leq 0, \quad (22d)$$

$$\mathbf{N}(\mathbf{u}) = 0, \quad (22e)$$

where \mathbf{F}_{1,\dots,N_M} are the N_M different models used to support the uncertainty, while \mathbf{F}_0 is a nominal model supporting the NMPC scheme. Trajectories $\mathbf{x}_{j,k}$ and $\mathbf{u}_{j,k}$ for $j = 1, \dots, N_M$ are the different models trajectories and the associated inputs. Functions ℓ_{1,\dots,N_M} , V_{1,\dots,N_M} the (possibly different) stage costs and terminal costs applying to the different models. The *non-anticipativity constraints* (22e) support the scenario-tree structure. For a given state \mathbf{s} and parameters θ , the NMPC scheme (22) delivers the input profiles

$$\mathbf{u}_j^*(\mathbf{s}, \theta) = \{ \mathbf{u}_{j,0}^*(\mathbf{s}, \theta), \dots, \mathbf{u}_{j,N}^*(\mathbf{s}, \theta) \}, \quad (23)$$

with $\mathbf{u}_{j,i}^*(\mathbf{s}, \theta) \in \mathbb{R}^{n_{\mathbf{a}}}$, and (22e) imposes

$$\mathbf{u}_0^*(\mathbf{s}, \theta) := \mathbf{u}_{i,0}^*(\mathbf{s}, \theta) = \mathbf{u}_{j,0}^*(\mathbf{s}, \theta), \quad \forall i, j. \quad (24)$$

As a result, the NMPC scheme (22) generates a parametrized deterministic policy according to:

$$\pi_\theta(\mathbf{s}) = \mathbf{u}_0^*(\mathbf{s}, \boldsymbol{\theta}) \in \mathbb{R}^{n_a}. \quad (25)$$

Policy π^s is implicitly deployed in (22) via the scenario tree. If the dispersion set \mathbf{X}_+ is known, the multiple models \mathbf{F}_{1,\dots,N_M} and terminal constraints (22d) can be chosen such that the robust NMPC scheme (22) delivers $\pi_\theta(\mathbf{s}) \in \mathbb{S}(\mathbf{s})$. Unfortunately, this selection can be difficult in general. We turn next to the robust linear MPC case, where this construction is much simpler.

B. Safe robust linear MPC

Exhaustively discussing the construction of the safe scenario tree in (22) for a given dispersion set $\mathbf{X}_+(\mathbf{s}, \mathbf{a})$ is beyond the scope of this paper. The process can be fairly involved, and we refer to [16], [2] for detailed discussions. For the sake of brevity, we will focus on the linear MPC case, whereby the MPC models \mathbf{F}_{1,\dots,N_M} and policy π^s are linear.

Let us consider the following outer approximation of the dispersion set \mathbf{X}_+ :

$$\mathbf{X}_+(\mathbf{s}, \mathbf{a}) \subseteq \mathbf{F}_0(\mathbf{s}, \mathbf{a}, \boldsymbol{\theta}) + \mathbf{W}, \quad \forall \mathbf{s}, \mathbf{a} \quad (26)$$

where we use a linear nominal model \mathbf{F}_0 and a polytope \mathbf{W} of vertices \mathbf{W}^{1,\dots,N_M} that can be construed as the extrema of a finite-support process noise, and which can be part (or functions of) the MPC parameters $\boldsymbol{\theta}$. For the sake of simplicity, we assume that \mathbf{W} is independent of the state-input pair \mathbf{s}, \mathbf{a} . The models \mathbf{F}_{1,\dots,N_M} can then be built based using:

$$\mathbf{F}_i = \mathbf{F}_0 + \mathbf{W}^i, \quad i = 1 \dots N_M \quad (27)$$

and using the linear policy:

$$\pi^s(\mathbf{x}_{j,k}, \mathbf{u}_{0,k}, \mathbf{x}_{0,k}) = \mathbf{u}_{0,k} - K(\mathbf{x}_{j,k} - \mathbf{x}_{0,k}) \quad (28)$$

where matrix K can be part (or function of) the MPC parameters $\boldsymbol{\theta}$. One can then verify by simple induction that:

$$\mathbf{X}_k(\mathbf{s}, \mathbf{a}, \pi^s) \subseteq \text{Conv}(\mathbf{x}_{1,k}, \dots, \mathbf{x}_{N_M,k}), \quad (29)$$

for $k = 0, \dots, N+1$, where Conv is the convex hull of the set of points $\mathbf{x}_{1,k}, \dots, \mathbf{x}_{N_M,k}$ solution of the MPC scheme (22). The terminal constraints (22d) ought then be constructed as, e.g., via the Robust Positive Invariant set corresponding to π^s in order to establish safety beyond the MPC horizon. For \mathbf{h}^s convex, the MPC scheme (22) delivers safe inputs [14], [13].

When the dispersion set $\mathbf{X}_+(\mathbf{s}, \mathbf{a})$ can only be inferred from data, condition (26) arguably translates to [5]:

$$\mathbf{s}_{k+1} - \mathbf{F}_0(\mathbf{s}_k, \mathbf{a}_k, \boldsymbol{\theta}) \in \mathbf{W}, \quad \forall (\mathbf{s}_{k+1}, \mathbf{s}_k, \mathbf{a}_k) \in \mathcal{D}, \quad (30)$$

where \mathcal{D} is the set of $N_{\mathcal{D}}$ observed state transitions. Condition (30) translates into a sample-based condition on the admissible parameters $\boldsymbol{\theta}$, i.e., it specifies the parameters that are safe with respect to the state transitions observed so far. Condition (30) tests whether the points $\mathbf{s}_{k+1} - \mathbf{F}_0(\mathbf{s}_k, \mathbf{a}_k, \boldsymbol{\theta})$ are in the polytope \mathbf{W} , which can be easily translated into a set of algebraic constraints imposed on $\boldsymbol{\theta}$. This observation will be used in Section III-B to build a safe RL-based learning.

We ought to underline here that building \mathbf{F}_0, \mathbf{W} based on (30) ensures the safety of the robust MPC scheme (22) only for an infinitely large, and sufficiently informative data set \mathcal{D} . In practice, using a finite data set entails that safety is ensured with a probability less than 1. The quantification of the probability of having a safe policy for a given, finite data set \mathcal{D} is beyond the scope of this paper, and is arguably best treated by means of the Information Field Theory [8]. The extension of the construction of a safe MPC presented in this section to the general NMPC case is theoretically feasible, but can be computationally intensive in practice. This aspect of the problem is beyond the scope if this paper.

IV. SAFE EXPLORATION

In this section, we investigate the deployment of the deterministic policy gradient method [17] when the input space is continuous and restricted by some safety constraints. We will show that in that case the classic tools used in the deterministic policy gradient method need some corrections.

In order to estimate the gradient of the advantage function $\nabla_{\mathbf{a}} A_{\pi_\theta}$, the inputs \mathbf{a} applied to the real system must differ from the actual policy $\pi_\theta(\mathbf{s})$, such that the advantage function $\hat{A}_{\pi_\theta}^{\mathbf{w}}(\mathbf{s}, \mathbf{a})$ is not trivially zero on the system trajectories, see (15). The exploration

$$\mathbf{e} := \mathbf{a} - \pi_\theta(\mathbf{s}), \quad (31)$$

is typically generated via selecting the inputs \mathbf{a} using a stochastic policy $\pi_\theta^\sigma[\mathbf{a} | \mathbf{s}]$, where σ relates to its covariance, having most of its mass in a neighborhood of $\pi_\theta(\mathbf{s})$. In the following, we will need the conditional mean and covariance of \mathbf{e} :

$$\boldsymbol{\eta}_{\mathbf{e}}(\mathbf{s}) = \mathbb{E}[\mathbf{e} | \mathbf{s}], \quad (32a)$$

$$\Sigma_{\mathbf{e}}(\mathbf{s}) = \mathbb{E}\left[(\mathbf{e} - \boldsymbol{\eta}_{\mathbf{e}})(\mathbf{e} - \boldsymbol{\eta}_{\mathbf{e}})^\top | \mathbf{s}\right]. \quad (32b)$$

The restriction of the exploration \mathbf{e} to yield inputs \mathbf{a} in the safe set $\mathbb{S}(\mathbf{s})$ can cause the exploration \mathbf{e} to not be centred, i.e., $\boldsymbol{\eta}_{\mathbf{e}} = 0$ may not hold, and the covariance $\Sigma_{\mathbf{e}}(\mathbf{s})$ can be restricted by the safe set. This observation is illustrated in Fig. 1, where the trivial static problem:

$$\pi_\theta = \arg \min_{\mathbf{u}} \frac{1}{2} \left\| \mathbf{u} - \begin{bmatrix} \boldsymbol{\theta}_1 \\ \boldsymbol{\theta}_2 \end{bmatrix} \right\|^2 \quad (33a)$$

$$\text{s.t.} \quad \|\mathbf{u}\|^2 \leq \boldsymbol{\theta}_3 \quad (33b)$$

was used, and the exploration generated via (46)-(47) detailed below.

The fact $\boldsymbol{\eta}_{\mathbf{e}}$ and $\Sigma_{\mathbf{e}}$ cannot be fully chosen in the presence of constraints ought to be accounted for when forming estimations of the gradient of the advantage function $\nabla_{\mathbf{a}} A_{\pi_\theta}$ in order to avoid biasing the estimation of the policy gradient (14). We develop next conditions on the exploration such that $\nabla_{\mathbf{a}} A_{\pi_\theta}$ can be estimated correctly.

A. Estimation of $\nabla_{\mathbf{a}} A_{\pi_\theta}$

A difficulty arises here when forming estimations of $\nabla_{\mathbf{a}} A_{\pi_\theta}$ using restricted explorations, which we detail hereafter. It

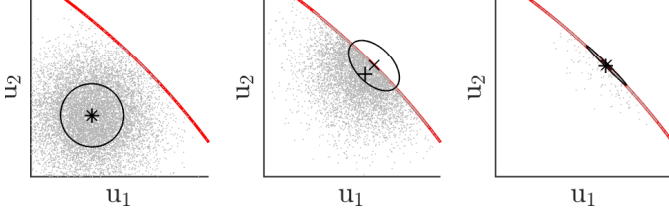


Fig. 1: Illustration of the mean (+ symbol) and covariance (ellipsoids) (32) of the exploration (31) subject to safety constraints (solid red line). The deterministic policy is depicted as the \times symbol, for the trivial problem (33), and different values of $\theta_{1,2}$ and $\theta_3 = 1$. Here the exploration is generated via (46)-(47) detailed below. One can observe that $\eta_e = 0$ is not possible to achieve when the policy is on the constraints, and that the covariances are impacted by the presence of the constraint. On the right-side graph, one can see how the covariance collapses when π_θ strongly activates the constraint.

is well known that estimating $\nabla_{\mathbf{a}} A_{\pi_\theta}$ directly is very difficult, hence one typically considers estimating the advantage function A_{π_θ} instead, from which the gradient $\nabla_{\mathbf{a}} A_{\pi_\theta}$ is evaluated. The estimation of the advantage function is carried by the function approximator $\hat{A}_{\pi_\theta}^{\mathbf{w}}$, parametrized by \mathbf{w} . One then seeks a solution to the least-squares problem [17]:

$$\mathbf{w} = \arg \min_{\mathbf{w}} \frac{1}{2} \mathbb{E}_{\pi_\theta^\sigma} \left[\left(Q_{\pi_\theta} - \hat{V}_{\pi_\theta} - \hat{A}_{\pi_\theta}^{\mathbf{w}} \right)^2 \right], \quad (34)$$

where the value function estimation $\hat{V}_{\pi_\theta} \approx V_{\pi_\theta}$ is a baseline supporting the evaluation of \mathbf{w} . Temporal-Difference or Monte Carlo techniques [18] are typically used to tackle (34). The policy gradient is then evaluated as:

$$\nabla_{\theta} \widehat{J}(\pi_\theta) = \mathbb{E}_{\pi_\theta^\sigma} \left[\nabla_{\theta} \pi_\theta \nabla_{\mathbf{a}} \hat{A}_{\pi_\theta}^{\mathbf{w}} \right]. \quad (35)$$

A compatible linear approximator $\hat{A}_{\pi_\theta}^{\mathbf{w}}$ is typically preferred, in order for (35) to match (14). In this paper, we propose to use the following function approximator inspired from [17]:

$$\hat{A}_{\pi_\theta}^{\mathbf{w}}(\mathbf{s}, \mathbf{a}) = \mathbf{w}^\top \nabla_{\theta} \pi_\theta M(\mathbf{a} - \pi_\theta - \mathbf{c}), \quad (36)$$

where M and \mathbf{c} are a (possibly) state-dependent $\mathbb{R}^{n_a \times n_a}$ symmetric matrix and \mathbb{R}^{n_a} vector. In [17], $M = I$ and $\mathbf{c} = 0$ is used but we will show in the following that we need in principle to make a different choice when the input is restricted to $\mathbb{S}(\mathbf{s})$. The following proposition delivers general conditions in order for (35) to match (14) when the exploration is restricted. Before delivering the Proposition, let us establish some key assumptions.

Assumption 1: The following hold:

- $Q_{\pi_\theta}(\mathbf{s}, \mathbf{a})$ is almost everywhere at least twice differentiable in \mathbf{a} on $\mathbb{S}(\mathbf{s})$ for all feasible \mathbf{s} , and its gradient with respect to \mathbf{a} are polynomially bounded.
- Stability assumption (7) holds.
- The MDP state probability density is bounded, i.e. it can not hold Dirac-like densities.
- \mathbf{e} results from the transformation of a Normal distribution via a polynomially bounded function

e. The following limits:

$$\lim_{\sigma \rightarrow 0} \frac{1}{\sigma} (\eta_e - \mathbf{c}) = 0 \quad (37a)$$

$$\lim_{\sigma \rightarrow 0} \frac{1}{\sigma} M \Sigma_e = I \quad (37b)$$

hold for all feasible \mathbf{s} .

Remark: We ought to underline here that assumptions 1a.-1d. are typically needed in RL algorithms, though often not explicitly stated. Assumption 1e. is not standard, and relates specifically to the problem of having restricted exploration. It essentially requires \mathbf{c} to be an asymptotic estimation of the exploration mean η_e and M to be a (scaled) asymptotic estimation of the inverse of the exploration covariance Σ_e . We should additionally observe that when the exploration is centred and isotropically distributed (i.e. $\eta_e = 0$, $\Sigma_e = \sigma I$), then $M = I$, $\mathbf{c} = 0$ satisfy (37), and the results found in [17] hold.

Proposition 1: Under Assumption 1, the deterministic policy gradient estimation (35) is asymptotically exact, i.e.

$$\lim_{\sigma \rightarrow 0} \nabla_{\theta} \widehat{J}(\pi_\theta) = \nabla_{\theta} J(\pi_\theta). \quad (38)$$

Proof: Using (36), the solution of the least-squares problem (34) satisfies the stationarity condition:

$$\mathbb{E}_{\pi_\theta^\sigma} \left[\nabla_{\theta} \pi_\theta M(\mathbf{e} - \mathbf{c}) \left(Q_{\pi_\theta} - \hat{V}_{\pi_\theta} - \hat{A}_{\pi_\theta}^{\mathbf{w}} \right) \right] = 0. \quad (39)$$

Since Q_{π_θ} is at least twice differentiable almost everywhere, its second-order expansion in \mathbf{a} at $\mathbf{e} = 0$ is valid almost everywhere, i.e.

$$\begin{aligned} Q_{\pi_\theta}(\mathbf{s}, \mathbf{a}) &= (V_{\pi_\theta} + \nabla_{\mathbf{a}} Q_{\pi_\theta}^\top (\mathbf{a} - \pi_\theta) + \xi)_{\mathbf{s}, \mathbf{a} = \pi_\theta} \\ &= V_{\pi_\theta}(\mathbf{s}) + \nabla_{\mathbf{a}} A_{\pi_\theta}(\mathbf{s}, \pi_\theta)^\top \mathbf{e} + \xi, \end{aligned} \quad (40)$$

where ξ is the second-order remainder of the Taylor expansion of Q_{π_θ} , and where we use $\nabla_{\mathbf{a}} Q_{\pi_\theta} = \nabla_{\mathbf{a}} A_{\pi_\theta}$, see (11). Because Q_{π_θ} is twice differentiable almost everywhere and using 1c., ξ is of order $\mathcal{O}(\|\mathbf{e}\|^2)$ almost everywhere. We then observe that (39) becomes:

$$\begin{aligned} \mathbb{E}_{\pi_\theta^\sigma} \left[\nabla_{\theta} \pi_\theta M(\mathbf{e} - \mathbf{c}) \mathbf{e}^\top \left(\nabla_{\mathbf{a}} A_{\pi_\theta} - \nabla_{\mathbf{a}} \hat{A}_{\pi_\theta}^{\mathbf{w}} \right) \right] \\ + \mathbb{E}_{\pi_\theta^\sigma} \left[\nabla_{\theta} \pi_\theta M(\mathbf{e} - \mathbf{c}) \xi \right] \\ + \mathbb{E}_{\pi_\theta^\sigma} \left[\nabla_{\theta} \pi_\theta M(\mathbf{e} - \mathbf{c}) \left(V_{\pi_\theta} - \hat{V}_{\pi_\theta} \right) \right] = 0. \end{aligned} \quad (41)$$

Function ξ is of second-order or more in \mathbf{e} and using the second assumption, it is polynomially bounded. Moreover, using assumption 1d., and using arguments from the Delta method [11], we can conclude that:

$$\lim_{\sigma \rightarrow 0} \frac{1}{\sigma} \mathbb{E} \left[\nabla_{\theta} \pi_\theta M(\mathbf{e} - \mathbf{c}) \xi | \mathbf{s} \right] = 0, \quad \forall \mathbf{s} \quad (42)$$

holds. It follows that the second term of (41) asymptotically vanishes faster than σ . Moreover, (37a) guarantees that the third term of (41) also asymptotically vanishes faster than σ . It follows that

$$\lim_{\sigma \rightarrow 0} \frac{1}{\sigma} \mathbb{E}_{\pi_\theta^\sigma} \left[\nabla_{\theta} \pi_\theta M(\mathbf{e} - \mathbf{c}) \mathbf{e}^\top \left(\nabla_{\mathbf{a}} A_{\pi_\theta} - \nabla_{\mathbf{a}} \hat{A}_{\pi_\theta}^{\mathbf{w}} \right) \right] = 0. \quad (43)$$

Using (37) we observe that using (37a):

$$\begin{aligned} & \lim_{\sigma \rightarrow 0} \frac{1}{\sigma} \mathbb{E} [M(\mathbf{e} - \mathbf{c}) \mathbf{e}^\top] \\ &= \lim_{\sigma \rightarrow 0} \frac{1}{\sigma} M (\Sigma_{\mathbf{e}} + \boldsymbol{\eta}_{\mathbf{e}} \boldsymbol{\eta}_{\mathbf{e}}^\top - \mathbf{c} \boldsymbol{\eta}_{\mathbf{e}}^\top) = \lim_{\sigma \rightarrow 0} \frac{1}{\sigma} M \Sigma_{\mathbf{e}}. \end{aligned} \quad (44)$$

We finally conclude that (39) and (43) with (35) entail that

$$\begin{aligned} & \lim_{\sigma \rightarrow 0} \frac{1}{\sigma} \mathbb{E}_{\pi_\theta^\sigma} \left[\nabla_{\boldsymbol{\theta}} \pi_\theta M \Sigma_{\mathbf{e}} \left(\nabla_{\mathbf{a}} A_{\pi_\theta} - \nabla_{\mathbf{a}} \hat{A}_{\pi_\theta}^{\mathbf{w}} \right) \right] \\ &= \mathbb{E}_{\pi_\theta} \left[\nabla_{\boldsymbol{\theta}} \pi_\theta \left(\nabla_{\mathbf{a}} A_{\pi_\theta} - \nabla_{\mathbf{a}} \hat{A}_{\pi_\theta}^{\mathbf{w}} \right) \right] = 0. \end{aligned} \quad (45)$$

where assumption (7) yields asymptotically the equivalence between $\mathbb{E}_{\pi_\theta^\sigma} [\cdot]$ and $\mathbb{E}_{\pi_\theta} [\cdot]$. Equation (38) follows. ■

We now turn to proposing a computationally effective method to generate a safe exploration and to compute mean and covariance estimations for \mathbf{e} , i.e., a matrix $M(\mathbf{s})$ and vector $\mathbf{c}(\mathbf{s})$ that satisfy conditions (37).

V. OPTIMIZATION-BASED SAFE EXPLORATION

In this section we proposed a modification of (20) allowing one to build a stochastic policy π_θ^σ that produces safe inputs for exploration, and for which the corrections M and \mathbf{c} satisfying Assumption 1e. are cheap to compute. The proposed approach will use the primal-dual interior-point method and techniques from parametric Nonlinear Programming. To that end we will consider inputs $\mathbf{a} = \mathbf{u}_0^{\mathbf{d}}(\mathbf{s}, \boldsymbol{\theta}, \mathbf{d})$ generated from:

$$\mathbf{u}^{\mathbf{d}}(\mathbf{s}, \boldsymbol{\theta}, \mathbf{d}) = \arg \min_{\mathbf{u}} \Phi^{\mathbf{d}}(\mathbf{x}, \mathbf{u}, \boldsymbol{\theta}, \mathbf{d}) \quad (46a)$$

$$\text{s.t. } \mathbf{f}(\mathbf{x}, \mathbf{u}, \mathbf{s}, \boldsymbol{\theta}) = 0, \quad (46b)$$

$$\mathbf{h}(\mathbf{x}, \mathbf{u}, \boldsymbol{\theta}) \leq 0, \quad (46c)$$

where $\Phi^{\mathbf{d}}(\mathbf{u}, \mathbf{s}, \boldsymbol{\theta}, \mathbf{d})$ is a modified version of the cost function Φ in (20), and $\mathbf{d} \in \mathbb{R}^{n_{\mathbf{a}}}$ is drawn from a Normal, centred probability distribution of density:

$$\mathbf{d} \sim \mathcal{N}(0, \sigma \Sigma(\mathbf{s})) \quad (47)$$

of covariance $\sigma \Sigma(\mathbf{s})$, where Σ (possibly) depends on \mathbf{s} . The stochastic policy π_θ^σ will then result from (46)-(47). A simple choice for $\Phi^{\mathbf{d}}(\mathbf{x}, \mathbf{u}, \boldsymbol{\theta}, \mathbf{d})$ is a gradient disturbance:

$$\Phi^{\mathbf{d}}(\mathbf{u}, \mathbf{s}, \boldsymbol{\theta}, \mathbf{d}) = \Phi(\mathbf{x}, \mathbf{u}, \boldsymbol{\theta}, \mathbf{d}) + \mathbf{d}^\top \mathbf{u}_0. \quad (48)$$

One can verify that $\mathbf{a} = \mathbf{u}_0^{\mathbf{d}}(\mathbf{s}, \boldsymbol{\theta}, \mathbf{d}) \in \mathbb{S}(\mathbf{s})$ by construction, such that the exploration is safe.

Deploying the principles detailed in Section II-B and Proposition 1 requires one to form at each time step asymptotically accurate estimations \mathbf{c} , M of the mean $\boldsymbol{\eta}_{\mathbf{e}}$ and covariance $\Sigma_{\mathbf{e}}$. For \mathbf{e} restricted to generate inputs in a non-trivial safe set $\mathbb{S}(\mathbf{s})$, estimating $\boldsymbol{\eta}_{\mathbf{e}}$ and $\Sigma_{\mathbf{e}}$ requires in general sampling the distribution of \mathbf{e} generated by (46)-(47), which is unfortunately computationally expensive as a large number of sample is required and each sample requires solving (46).

An alternative to estimating $\boldsymbol{\eta}_{\mathbf{e}}$ and $\Sigma_{\mathbf{e}}$ using sampling is to form these estimations via a Taylor expansion of $\mathbf{u}_0^{\mathbf{d}}(\mathbf{s}, \boldsymbol{\theta}, \mathbf{d})$ in \mathbf{d} . Unfortunately, $\mathbf{u}_0^{\mathbf{d}}(\mathbf{s}, \boldsymbol{\theta}, \mathbf{d})$ is in general non-smooth due to the presence of inequality constraints in (46). To alleviate this problem, in this section, we propose to cast (46) in a primal-dual interior point formulation, i.e., we consider that

the solutions of (46) are obtained from solving the relaxed Karush-Kuhn-Tucker (KKT) conditions [7]:

$$\mathbf{r}_\tau(\mathbf{z}, \boldsymbol{\theta}, \mathbf{d}) = \begin{bmatrix} \nabla_{\mathbf{w}} \Phi^{\mathbf{d}} + \nabla_{\mathbf{w}} \mathbf{h} \boldsymbol{\mu} + \nabla_{\mathbf{w}} \mathbf{f} \boldsymbol{\lambda} \\ \mathbf{f} \\ \text{diag}(\boldsymbol{\mu}) \mathbf{h} + \tau \end{bmatrix} = 0, \quad (49)$$

for $\tau > 0$, and under the conditions $\mathbf{h} < 0$ and $\boldsymbol{\mu} > 0$. Here $\boldsymbol{\mu}, \boldsymbol{\lambda}$ are the multipliers associated to the equality and inequality constraints in (46), and we label $\mathbf{w} = \{\mathbf{x}, \mathbf{u}\}$ and $\mathbf{z} = \{\mathbf{w}, \boldsymbol{\lambda}, \boldsymbol{\mu}\}$ the primal-dual variables of (49). We will label $\mathbf{u}^\tau(\mathbf{s}, \boldsymbol{\theta}, \mathbf{d})$ the parametric primal solution of (49).

The error between the true solution of (46) and the one delivered by solving (49) is of the order of the relaxation parameter τ , and the solution $\mathbf{u}^\tau(\mathbf{s}, \boldsymbol{\theta}, \mathbf{d})$ is guaranteed to satisfy the constraints of (46) for all $\tau \geq 0$, hence (49) delivers safe policies if (46) does. The relaxed KKT conditions (49) yield a smooth function $\mathbf{u}^\tau(\mathbf{s}, \boldsymbol{\theta}, \mathbf{d})$, such that its Taylor expansion is well-defined everywhere. The relaxed KKT conditions (49) will be used next to generate the safe exploration, and the deterministic policy:

$$\pi_\theta^\tau = \mathbf{u}_0^\tau(\mathbf{s}, \boldsymbol{\theta}, \mathbf{0}). \quad (50)$$

A. Covariance and mean estimators

For the sake of clarity, let us use the short notation $\mathbf{g}(\mathbf{s}, \boldsymbol{\theta}, \mathbf{d}) := \mathbf{u}_0^\tau(\mathbf{s}, \boldsymbol{\theta}, \mathbf{d})$. Hence \mathbf{g} is evaluated by solving (49) and extracting the first control input $\mathbf{u}_0^\tau \in \mathbb{R}^{n_{\mathbf{a}}}$. This function will be instrumental in building cheap mean and covariance estimators satisfying (37). Let us provide these estimators in the following Proposition.

Proposition 2: If $\mathbf{u}^{\mathbf{d}}(\mathbf{s}, \boldsymbol{\theta}, \mathbf{d})$ arising from NLP (46) is polynomially bounded in \mathbf{d} , then the following mean and covariance estimators:

$$\mathbf{c} = \frac{1}{2} \sum_{i,j=1}^{n_{\mathbf{a}}} \frac{\partial^2 \mathbf{g}}{\partial \mathbf{d}_i \partial \mathbf{d}_j} \Sigma_{ij}, \quad (51a)$$

$$M = \left(\frac{\partial \mathbf{g}}{\partial \mathbf{d}} \Sigma \frac{\partial \mathbf{g}^\top}{\partial \mathbf{d}} \right)_{\mathbf{d}=\mathbf{0}}^{-1} \quad (51b)$$

satisfy conditions (37), where Σ is used in (47).

Proof: We observe that:

$$\begin{aligned} \boldsymbol{\eta}_{\mathbf{e}} &= \mathbb{E} [\mathbf{g}(\mathbf{s}, \boldsymbol{\theta}, \mathbf{d}) - \mathbf{g}(\mathbf{s}, \boldsymbol{\theta}, \mathbf{0})] \\ &= \mathbb{E} \left[\frac{\partial \mathbf{g}}{\partial \mathbf{d}} \Big|_{\mathbf{d}=\mathbf{0}} \mathbf{d} + \frac{1}{2} \sum_{i,j=1}^{n_{\mathbf{a}}} \frac{\partial^2 \mathbf{g}}{\partial \mathbf{d}_i \partial \mathbf{d}_j} \mathbf{d}_i \mathbf{d}_j + \boldsymbol{\varsigma} \right], \end{aligned} \quad (52)$$

where $\boldsymbol{\varsigma}$ is the third-order remainder of the expansion of \mathbf{g} . We observe that since \mathbf{d} has zero mean (52) becomes:

$$\boldsymbol{\eta}_{\mathbf{e}} = \frac{\sigma}{2} \sum_{i,j=1}^{n_{\mathbf{a}}} \frac{\partial^2 \mathbf{g}}{\partial \mathbf{d}_i \partial \mathbf{d}_j} \Sigma_{ij} + \mathbb{E} [\boldsymbol{\varsigma}]. \quad (53)$$

We also observe that $\mathbb{E} [\boldsymbol{\varsigma}] = \mathcal{O}(\sigma^2)$ holds using arguments from the Delta method [11]. It follows that (51a) satisfies (37a). Furthermore, we observe that

$$\Sigma_{\mathbf{e}} = \mathbb{E} [\mathbf{e} \mathbf{e}^\top] - \boldsymbol{\eta}_{\mathbf{e}} \boldsymbol{\eta}_{\mathbf{e}}^\top, \quad (54)$$

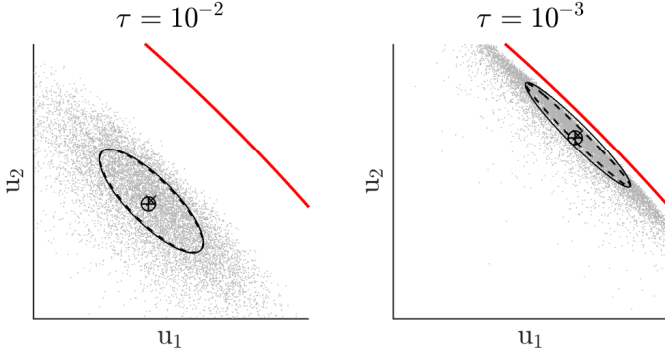


Fig. 2: Illustration of the mean and covariance (32) of the exploration (31) subject to safety constraints (solid red line here), generated by the interior-point approach (49) for two value of the relaxation parameter τ . The policy is generated by (33), and the exploration by (46)-(48), with $\Sigma = I$. The mean estimator \mathbf{c} (+ symbol) and covariance estimator M^{-1} (dashed ellipsoid) (51) are compared to the ones estimated by sampling (o symbol, solid line ellipsoid).

and that:

$$\mathbb{E}[\mathbf{e}\mathbf{e}^\top] = \sigma \left. \frac{\partial \mathbf{g}}{\partial \mathbf{d}} \Sigma \frac{\partial \mathbf{g}^\top}{\partial \mathbf{d}} \right|_{\mathbf{d}=0} + \mathcal{O}(\sigma^2), \quad (55)$$

holds using similar arguments as for (52)-(53). It follows that:

$$\lim_{\sigma \rightarrow 0} \frac{1}{\sigma} M \Sigma \mathbf{e} = \left(\frac{\partial \mathbf{g}}{\partial \mathbf{d}} \Sigma \frac{\partial \mathbf{g}^\top}{\partial \mathbf{d}} \right)^{-1} \left(\frac{\partial \mathbf{g}}{\partial \mathbf{d}} \Sigma \frac{\partial \mathbf{g}^\top}{\partial \mathbf{d}} \right) = I, \quad (56)$$

where the Jacobians are evaluated at $\mathbf{d} = 0$. ■

Note that deploying (51b) requires the Jacobian $\frac{\partial \mathbf{g}}{\partial \mathbf{d}} \in \mathbb{R}^{n_a \times n_a}$ to be full rank. This Jacobian also appears in [10] to develop the stochastic policy gradient counterpart of this paper, and its rank is investigated. We will not repeat in detail this analysis here, but let us recall its conclusion: for the choice of cost function (48), the Jacobian $\frac{\partial \mathbf{g}}{\partial \mathbf{d}}$ is full rank for any $\tau > 0$ if the NLP (46) satisfies the Linearly Independent Constraint Qualification (LICQ) and the Second-Order Sufficient Condition (SOSC). However, $\frac{\partial \mathbf{g}}{\partial \mathbf{d}}$ can tend to a rank deficient matrix for $\tau \rightarrow 0$ if \mathbf{u}_0^d delivered by (46) activates some of the inequality constraints (46c).

Similarly to what has been reported in [10], this issue disappears in some specific cases, which are discussed in the following Proposition, and illustrated in Fig. 3 below.

Proposition 3: For the choice of cost function (48), and if the MPC model dynamics and constraints are not depending on the parameters, i.e. $\nabla_{\theta} \mathbf{h} = 0$, $\nabla_{\theta} \mathbf{f} = 0$, then the choice of M , \mathbf{c} proposed by (51) yields (38) for $\tau \rightarrow 0$ if problem (46) fulfils LICQ and SOSC.

Proof: We will prove this statement in an active-set setting deployed on (46), with (51b) evaluated via a pseudo-inverse. The statement of the Proposition will then hold from the convergence of the Interior-Point solution to the active-set one. We will then investigate (44)-(45) in that context. Using (51b) with a pseudo-inverse, and using similar developments

as in Proposition (1), one can verify that:

$$\begin{aligned} \lim_{\sigma \rightarrow 0} \frac{1}{\sigma} \mathbb{E}[\nabla_{\theta} \pi_{\theta} M (\mathbf{e} - \mathbf{c}) \mathbf{e}^\top] & \quad (57) \\ &= \nabla_{\theta} \pi_{\theta} \left(\frac{\partial \mathbf{g}}{\partial \mathbf{d}} \Sigma \frac{\partial \mathbf{g}^\top}{\partial \mathbf{d}} \right)^+ \left(\frac{\partial \mathbf{g}}{\partial \mathbf{d}} \Sigma \frac{\partial \mathbf{g}^\top}{\partial \mathbf{d}} \right) \\ &= \left(\frac{\partial \mathbf{g}}{\partial \mathbf{d}} \Sigma \frac{\partial \mathbf{g}^\top}{\partial \mathbf{d}} \right)^+ \left(\frac{\partial \mathbf{g}}{\partial \mathbf{d}} \Sigma \frac{\partial \mathbf{g}^\top}{\partial \mathbf{d}} \right) \frac{\partial \mathbf{g}}{\partial \theta}. \end{aligned}$$

We will then prove that under the assumptions of this Proposition, $\frac{\partial \mathbf{g}}{\partial \theta}$ is in the range space of $\frac{\partial \mathbf{g}}{\partial \mathbf{d}} \Sigma \frac{\partial \mathbf{g}^\top}{\partial \mathbf{d}}$, such that

$$\left(\frac{\partial \mathbf{g}}{\partial \mathbf{d}} \Sigma \frac{\partial \mathbf{g}^\top}{\partial \mathbf{d}} \right)^+ \left(\frac{\partial \mathbf{g}}{\partial \mathbf{d}} \Sigma \frac{\partial \mathbf{g}^\top}{\partial \mathbf{d}} \right) \frac{\partial \mathbf{g}}{\partial \theta} = \frac{\partial \mathbf{g}}{\partial \theta} \quad (58)$$

holds. To that end, consider \mathbb{A} the (strictly) active set of (46), i.e., the set of indices i such that $\mathbf{h}_i = 0$, $\mu_i > 0$ at the solution. We observe that

$$\begin{bmatrix} H & \nabla_{\mathbf{w}} \mathbf{q} \\ \nabla_{\mathbf{w}} \mathbf{q}^\top & 0 \end{bmatrix} \begin{bmatrix} \frac{\partial \mathbf{w}}{\partial \mathbf{d}} \\ \frac{\partial \mu}{\partial \mathbf{d}} \end{bmatrix} = - \begin{bmatrix} \nabla_{\mathbf{w}d} \Phi^d \\ 0 \end{bmatrix}, \quad (59)$$

where H is the Hessian of the Lagrange function associated to (46) and

$$\mathbf{q} = \begin{bmatrix} \mathbf{f} \\ \mathbf{h}_{\mathbb{A}} \end{bmatrix}, \quad \boldsymbol{\nu} = \begin{bmatrix} \boldsymbol{\lambda} \\ \boldsymbol{\mu}_{\mathbb{A}} \end{bmatrix}. \quad (60)$$

Defining $\mathcal{N}_{\mathbb{A}}$ the null space of $\nabla_{\mathbf{w}} \mathbf{q}^\top$, i.e. $\nabla_{\mathbf{w}} \mathbf{q}^\top \mathcal{N}_{\mathbb{A}} = 0$, we observe that:

$$\frac{\partial \mathbf{g}}{\partial \mathbf{d}} = -\mathcal{N}_{\mathbb{A}_0} (\mathcal{N}_{\mathbb{A}}^\top H \mathcal{N}_{\mathbb{A}})^{-1} \mathcal{N}_{\mathbb{A}_0}^\top, \quad (61)$$

where $\mathcal{N}_{\mathbb{A}_0} = [I_{n_a \times n_a} \ 0 \ \dots \ 0] \mathcal{N}_{\mathbb{A}}$. Using a similar reasoning, and since $\frac{\partial \nabla_{\mathbf{w}} \mathbf{q}}{\partial \theta} = 0$, we observe that:

$$\frac{\partial \mathbf{g}}{\partial \theta} = -\mathcal{N}_{\mathbb{A}_0} (\mathcal{N}_{\mathbb{A}}^\top H \mathcal{N}_{\mathbb{A}})^{-1} \mathcal{N}_{\mathbb{A}}^\top \nabla_{\mathbf{w}\theta} \Phi, \quad (62)$$

such that $\frac{\partial \mathbf{g}}{\partial \theta}$ is in the range space of $\frac{\partial \mathbf{g}}{\partial \mathbf{d}}$. As a result, for Σ full rank $\frac{\partial \mathbf{g}}{\partial \theta}$ is in the range space of $\frac{\partial \mathbf{g}}{\partial \mathbf{d}} \Sigma \frac{\partial \mathbf{g}^\top}{\partial \mathbf{d}}$, such that (58) holds. Using (51b) defined via the pseudo-inverse, and (44), (53)-(55) one can observe that:

$$\begin{aligned} \lim_{\sigma \rightarrow 0} \frac{1}{\sigma} \mathbb{E}[\nabla_{\theta} \pi_{\theta} M (\mathbf{e} - \mathbf{c}) \mathbf{e}^\top] & \quad (63) \\ &= \mathbb{E} \left[\nabla_{\theta} \pi_{\theta} M \left(\frac{\partial \mathbf{g}}{\partial \mathbf{d}} \Sigma \frac{\partial \mathbf{g}^\top}{\partial \mathbf{d}} \right) \right] \end{aligned}$$

holds. Using (58), we finally observe that

$$\lim_{\sigma \rightarrow 0} \frac{1}{\sigma} \mathbb{E}[\nabla_{\theta} \pi_{\theta} M (\mathbf{e} - \mathbf{c}) \mathbf{e}^\top] = \nabla_{\theta} \pi_{\theta}. \quad (64)$$

We can then conclude that (45) holds and that the policy gradient estimator is exact, i.e. (38) holds. ■

We need to caveat here the practical implications of Proposition 3. First, the results hold for $\tau \rightarrow 0$, with $\sigma \rightarrow 0$. If using matrix M defined via the classic inverse (51a), the results of Proposition 3 hold in the sense that for any τ , (64) holds asymptotically for σ sufficiently small. Hence reducing τ may require reducing σ for (64) to hold. Alternatively, M ought to

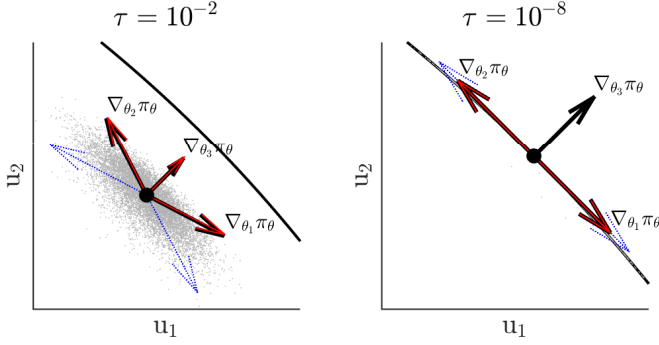


Fig. 3: Illustration of Proposition 3 and the following discussion for the small problem (33). The solid black arrows represent the directions spanned by $\nabla_{\theta}\pi_{\theta}$. The red, dashed-line arrows report the corresponding terms in $\frac{1}{\sigma}\mathbb{E}[\nabla_{\theta}\pi_{\theta}M(\mathbf{e}-\mathbf{c})\mathbf{e}^{\top}]$ appearing in (64). The dotted-line blue arrows report the directions spanned by $\frac{\partial\mathbf{g}}{\partial\mathbf{d}}$. One can see that (64) holds for $\tau > 0$ (left graph), and holds for parameters $\theta_{1,2}$ for $\tau \rightarrow 0$ (right graph) as they satisfy the assumptions of Proposition 3. However, (64) does not hold for θ_3 , as it influences the constraint (33b), and therefore violates the assumptions of Proposition 3 (right graph). One can construe the problem as a lack of exploration (blue dotted-line arrows) in the direction $\nabla_{\theta_3}\pi_{\theta}$ due to the active constraint.

be systematically defined via a pseudo-inverse. Unfortunately, the definition of M then becomes somewhat arbitrary and non-smooth.

Additionally, one ought to observe that the assumptions of Proposition 3 are fairly restrictive, as they do not allow one to adjust the model or constraints in the robust MPC scheme, which leaves only the cost function as subject to adaptation. While [9] shows that it is theoretically enough to adapt only the MPC cost function to generate the optimal control policy from the MPC scheme, this result requires a rich parametrization of the cost, which may be undesirable.

When the model and/or constraints of the NMPC scheme are meant to be adjusted by the RL algorithm, such that the assumptions of Proposition 3 are not satisfied, then the policy gradient can be incorrect. The issue is associated to parameters θ that can (locally) move the policy in directions orthogonal to the strictly active constraints. Indeed, for $\tau \rightarrow 0$, (46)-(48) yield samples that are (for $\sigma \rightarrow 0$) in the span of $\frac{\partial\mathbf{g}}{\partial\mathbf{d}}$, which is rank deficient when π_{θ} strictly activates some constraints. However, if the assumptions of Proposition 3 are not satisfied, $\frac{\partial\mathbf{g}}{\partial\theta}$ can span directions that are in the null space of $\frac{\partial\mathbf{g}}{\partial\mathbf{d}}$, and therefore not explored. It follows that the policy gradient can be wrong in these directions. These observations are illustrated in Fig. 3.

For cases that do not satisfy the assumptions of Proposition 3, working with $\tau > 0$ (although possibly small) appears to be the best option. We ought to underline here that while the corrections M and \mathbf{c} are in theory needed in order to build a correct policy gradient estimation (38), the error in the policy gradient estimation resulting from not using these corrections is yet to be investigated in detail.

While Σ in (47) can in principle be chosen freely, a reasonable option is to adopt $\Sigma = I$, i.e., an isotropic gradient

disturbance, in which case

$$M = \left(\frac{\partial\mathbf{g}}{\partial\mathbf{d}} \frac{\partial\mathbf{g}}{\partial\mathbf{d}}^{\top} \right)_{\mathbf{d}=0}^{-1}. \quad (65)$$

We turn now to detailing how (51) can be evaluated at low computational expenses.

B. Implementation & Sensitivity computation

In order to compute the sensitivities required in (51) to evaluate \mathbf{c} and M , the first and second-order sensitivities of \mathbf{g} are required. In turn, this requires one to evaluate the sensitivities of the relaxed KKTs (49). In this section we detail how this can be done. We first observe that if LICQ and SOSC hold [15] for the NLP (46), then $\frac{\partial\mathbf{r}_{\tau}}{\partial\mathbf{z}}$ is full rank, and the Implicit Function Theorem (IFT) guarantees that one can evaluate the first-order sensitivities of (49) by solving the linear equations:

$$\frac{\partial\mathbf{r}_{\tau}}{\partial\mathbf{z}} \frac{\partial\mathbf{z}}{\partial\mathbf{d}} + \frac{\partial\mathbf{r}_{\tau}}{\partial\mathbf{d}} = 0, \quad \frac{\partial\mathbf{r}_{\tau}}{\partial\mathbf{z}} \frac{\partial\mathbf{z}}{\partial\theta} + \frac{\partial\mathbf{r}_{\tau}}{\partial\theta} = 0, \quad (66)$$

for $\frac{\partial\mathbf{z}}{\partial\mathbf{d}}$ and $\frac{\partial\mathbf{z}}{\partial\theta}$. One can then readily obtain $\frac{\partial\mathbf{g}}{\partial\mathbf{d}}$ and $\frac{\partial\mathbf{g}}{\partial\theta}$ by extracting the first $n_{\mathbf{a}}$ rows of $\frac{\partial\mathbf{z}}{\partial\mathbf{d}}$, $\frac{\partial\mathbf{z}}{\partial\theta}$. The Jacobian $\frac{\partial\mathbf{g}}{\partial\theta}$ the delivers

$$\nabla_{\theta}\pi_{\theta}^{\tau} = \frac{\partial\mathbf{g}}{\partial\theta}^{\top}, \quad (67)$$

required in (35), while $\frac{\partial\mathbf{g}}{\partial\mathbf{d}}$ is required in (51b).

The second-order term $\frac{\partial^2\mathbf{g}}{\partial\mathbf{d}_i\partial\mathbf{d}_j}$ needed in (51a) can be obtained from solving the second-order sensitivity equation of the NLP:

$$\begin{aligned} \frac{\partial\mathbf{r}_{\tau}}{\partial\mathbf{z}} \frac{\partial^2\mathbf{z}}{\partial\mathbf{d}_i\partial\mathbf{d}_j} + \left(\frac{\partial^2\mathbf{r}_{\tau}}{\partial\mathbf{d}_i\partial\mathbf{z}} + \sum_k \frac{\partial^2\mathbf{r}_{\tau}}{\partial\mathbf{z}\partial\mathbf{z}_k} \frac{\partial\mathbf{z}_k}{\partial\mathbf{d}_i} \right) \frac{\partial\mathbf{z}}{\partial\mathbf{d}_j} + \frac{\partial^2\mathbf{r}_{\tau}}{\partial\mathbf{d}_i\partial\mathbf{d}_j} \\ + \sum_k \frac{\partial^2\mathbf{r}_{\tau}}{\partial\mathbf{d}_j\partial\mathbf{z}_k} \frac{\partial\mathbf{z}_k}{\partial\mathbf{d}_i} = 0, \end{aligned} \quad (68)$$

for $\frac{\partial^2\mathbf{z}}{\partial\mathbf{d}_i\partial\mathbf{d}_j}$. The sensitivity $\frac{\partial^2\mathbf{g}}{\partial\mathbf{d}_i\partial\mathbf{d}_j}$ is then obtained by extracting the first $n_{\mathbf{a}}$ rows of $\frac{\partial^2\mathbf{z}}{\partial\mathbf{d}_i\partial\mathbf{d}_j}$. Note that for computational efficiency, (68) is best treated as a tensor. We should underline here that computing the sensitivities is typically fairly inexpensive, if using an adequate algorithmic.

VI. SAFE RL STEPS FOR ROBUST LINEAR MPC

The methodology described so far allows one to deploy a safe policy and safe exploration using a robust NMPC scheme in order to compute the deterministic policy gradient, and determine directions in the parameter space θ that improve the closed-loop performance of the NMPC scheme. However, taking a step in θ can arguably jeopardize the safety of the NMPC scheme itself, e.g., by modifying the constraints, or the models underlying the scenario tree. The problem of modifying the NMPC parameters while maintaining safety is arguably a complex one, and beyond the scope of this paper. However, in this section, we propose a practical approach to handle this problem in a data-driven context. In this paper,

we propose an approach readily applicable to the linear robust MPC case, see Section III-B.

When the dispersion set $\mathbf{X}_+(\mathbf{s}, \mathbf{a})$ can only be inferred from data, condition (26) arguably translates to (30). Condition (30) translates into a condition on the admissible parameters $\boldsymbol{\theta}$, i.e., it specifies the parameters that are safe *with respect to the data observed so far*. Condition (30) tests whether the points $\mathbf{s}_{k+1} - \mathbf{F}_0(\mathbf{s}_k, \mathbf{a}_k, \boldsymbol{\theta})$ are in the polytope \mathbf{W} , which can be easily translated into a set of algebraic constraints imposed on $\boldsymbol{\theta}$. We observe that a classic gradient step of step-size $\alpha > 0$ reads as:

$$\boldsymbol{\theta} = \boldsymbol{\theta}_- - \alpha \nabla_{\boldsymbol{\theta}} \widehat{J}(\boldsymbol{\pi}_{\boldsymbol{\theta}}), \quad (69)$$

where $\boldsymbol{\theta}_-$ is the previous vector of parameters. One can observe that the gradient step can be construed as the solution of the optimization problem:

$$\min_{\boldsymbol{\theta}} \frac{1}{2} \|\boldsymbol{\theta} - \boldsymbol{\theta}_-\|^2 + \alpha \nabla_{\boldsymbol{\theta}} \widehat{J}(\boldsymbol{\pi}_{\boldsymbol{\theta}})^\top (\boldsymbol{\theta} - \boldsymbol{\theta}_-). \quad (70)$$

Imposing (30) on the gradient step generating the new parameters can then be cast as the following constrained optimization problem:

$$\min_{\boldsymbol{\theta}, \boldsymbol{\vartheta}} \frac{1}{2} \|\boldsymbol{\theta} - \boldsymbol{\theta}_-\|^2 + \alpha \nabla_{\boldsymbol{\theta}} \widehat{J}(\boldsymbol{\pi}_{\boldsymbol{\theta}})^\top (\boldsymbol{\theta} - \boldsymbol{\theta}_-) \quad (71a)$$

$$\text{s.t. } \mathbf{s}_{k+1} - \mathbf{F}_0(\mathbf{s}_k, \mathbf{a}_k, \boldsymbol{\theta}) - \sum_{i=1}^V \sum_{k=0}^{N_{\mathcal{D}}} \boldsymbol{\vartheta}_{i,k} \mathbf{W}^i = 0, \quad (71b)$$

$$\sum_{i=1}^V \boldsymbol{\vartheta}_{i,k} = 1, \quad \forall k = 0, \dots, N_{\mathcal{D}}, \quad (71c)$$

$$\boldsymbol{\vartheta}_{i,k} \geq 0 \quad \forall k = 0, \dots, N_{\mathcal{D}}, \quad i = 1, \dots, V, \quad (71d)$$

where (71b)-(71d) are the algebraic conditions testing (30). We observe that unfortunately the complexity of (71) grows with the amount of data $N_{\mathcal{D}}$ in use. In practice, the data set \mathcal{D} should arguably be limited to incorporate relevant state transitions. A data compression technique has been proposed in [20] to alleviate this issue in the case the nominal model \mathbf{F}_0 is fixed. Future work will improve on this baseline.

VII. IMPLEMENTATION & ILLUSTRATIVE EXAMPLE

In this section, we provide some details on how the principle presented in this paper can be implemented, and provide an illustrative example of this implementation. At each time instant k , for a given state \mathbf{s}_k , the deterministic policy $\boldsymbol{\pi}_{\boldsymbol{\theta}}$ is computed according to (49) with $\mathbf{d} = 0$. The solution is used to build M and \mathbf{c} . The exploration is then generated according to (49) with \mathbf{d} drawn from (47). We ought to underline here that, unfortunately, the NLP has to be solved twice. The data are then collected to perform the estimations (34) and (35) either on-the-fly or in a batch fashion. The policy gradient estimation (35) is then used to compute the safe parameter update according to (71).

A. RL approach

In the example below, a batch RL method has been used. The policy gradient was evaluated using batch Least-Squares

Temporal-Difference (LSTD) techniques, whereby for each evaluation, the closed-loop system is run S times for N_t time steps, generating S trajectory samples of duration N_t . The value function estimations is constructed using:

$$\sum_{k=0}^{N_t} \sum_{i=1}^S \delta^V(\mathbf{s}_{k,i}, \mathbf{a}_{k,i}, \mathbf{s}_{k+1,i}) \nabla_{\mathbf{v}} \hat{V}_{\boldsymbol{\pi}_{\boldsymbol{\theta}}}^{\mathbf{v}}(\mathbf{s}_{k,i}) = 0 \quad (72a)$$

$$\delta^V := L(\mathbf{s}_{k,i}, \mathbf{a}_{k,i}) + \gamma \hat{V}_{\boldsymbol{\pi}_{\boldsymbol{\theta}}}^{\mathbf{v}}(\mathbf{s}_{k+1,i}) - \hat{V}_{\boldsymbol{\pi}_{\boldsymbol{\theta}}}^{\mathbf{v}}(\mathbf{s}_{k,i}) \quad (72b)$$

and based on a linear value function approximation

$$\hat{V}_{\boldsymbol{\pi}_{\boldsymbol{\theta}}}^{\mathbf{v}}(\mathbf{s}) = \boldsymbol{\varrho}(\mathbf{s})^\top \mathbf{v}. \quad (73)$$

A simple fully parametrized quadratic function in \mathbf{s} to build $\hat{V}_{\boldsymbol{\pi}_{\boldsymbol{\theta}}}^{\mathbf{v}}$ in the example below. Using the parameters \mathbf{v} obtained from (72), the advantage function estimation is given by:

$$\sum_{k=0}^{N_t} \sum_{i=1}^S \delta^Q(\mathbf{s}_{k,i}, \mathbf{a}_{k,i}, \mathbf{s}_{k+1,i}) \nabla_{\mathbf{w}} \hat{Q}_{\boldsymbol{\pi}_{\boldsymbol{\theta}}}^{\mathbf{w}}(\mathbf{s}_{k,i}, \mathbf{a}_{k,i}) = 0, \quad (74a)$$

$$\delta^Q := L(\mathbf{s}_{k,i}, \mathbf{a}_{k,i}) + \gamma \hat{V}_{\boldsymbol{\pi}_{\boldsymbol{\theta}}}^{\mathbf{v}}(\mathbf{s}_{k+1,i}) - \hat{Q}_{\boldsymbol{\pi}_{\boldsymbol{\theta}}}^{\mathbf{w}}(\mathbf{s}_{k,i}, \mathbf{a}_{k,i}), \quad (74b)$$

$$\hat{Q}_{\boldsymbol{\pi}_{\boldsymbol{\theta}}}^{\mathbf{w}}(\mathbf{s}_{k,i}, \mathbf{a}_{k,i}) = \hat{V}_{\boldsymbol{\pi}_{\boldsymbol{\theta}}}^{\mathbf{v}}(\mathbf{s}_{k,i}) + \hat{A}_{\boldsymbol{\pi}_{\boldsymbol{\theta}}}^{\mathbf{w}}(\mathbf{s}_{k,i}, \mathbf{a}_{k,i}), \quad (74c)$$

where $\hat{A}_{\boldsymbol{\pi}_{\boldsymbol{\theta}}}^{\mathbf{w}}$ is based on (36). We observe that both (72) and (74) are linear in the parameters \mathbf{v} and \mathbf{w} , and therefore straightforward to solve. However, they can be ill-posed on some data sets, and they ought to be solved using, e.g., a Moore-Penrose pseudo-inverse, preferably with a reasonably large saturation of the lowest singular value. The policy gradient estimation is then obtained from (35), using:

$$\nabla_{\boldsymbol{\theta}} \widehat{J}(\boldsymbol{\pi}_{\boldsymbol{\theta}}) = \sum_{k=0}^{N_t} \sum_{i=1}^S \nabla_{\boldsymbol{\theta}} \boldsymbol{\pi}_{\boldsymbol{\theta}}(\mathbf{s}_{k,i}) M(\mathbf{s}_{k,i}) \nabla_{\boldsymbol{\theta}} \boldsymbol{\pi}_{\boldsymbol{\theta}}(\mathbf{s}_{k,i})^\top \mathbf{w}. \quad (75)$$

B. Robust linear MPC scheme

While the proposed theory is not limited to linear problems, for the sake of clarity, we propose to use a fairly simple robust linear MPC example using multiple models and process noise. We will consider the policy as delivered by the following robust MPC scheme based on multiple models and a linear feedback policy:

$$\min_{\mathbf{u}, \mathbf{x}} \sum_{j=0}^{N_M} \left(\|\mathbf{x}_{j,N} - \bar{\mathbf{x}}\|^2 + \sum_{k=0}^{N-1} \left\| \begin{bmatrix} \mathbf{x}_{j,k} - \bar{\mathbf{x}} \\ \mathbf{u}_{j,k} - \bar{\mathbf{u}} \end{bmatrix} \right\|^2 \right) \quad (76a)$$

$$\text{s.t. } \mathbf{x}_{j,k+1} = A_0 \mathbf{x}_{j,k} + B_0 \mathbf{u}_{j,k} + \mathbf{b}_0 + \mathbf{W}^j, \quad (76b)$$

$$\|\mathbf{x}_{j,k}\|^2 \leq 1, \quad \forall j = 0, \dots, N_M, k = 1, \dots, N, \quad (76c)$$

$$\mathbf{x}_{j,0} = \mathbf{s}, \quad \forall j = 1, \dots, N_M, \quad (76d)$$

$$\mathbf{u}_{j,0} = \mathbf{u}_{k,0}, \quad \forall k, j = 0, \dots, N_M, \quad (76e)$$

$$\mathbf{u}_{j,k} = \mathbf{u}_{0,k} - K(\mathbf{x}_{j,k} - \mathbf{x}_{0,k}), \quad j = 1, \dots, N_M, \quad (76f)$$

where A_0, B_0, \mathbf{b}_0 yield the MPC nominal model corresponding to \mathbf{F}_0 , with $\mathbf{W}^0 = 0$, and $\mathbf{W}^{1, \dots, M}$ capture the vertices of the dispersion set outer approximation. Hence model $j = 0$ serves as nominal model and models $j = 1, \dots, N_M$ capture the state dispersion over time. The linear feedback matrix K is possibly part of the MPC parameters $\boldsymbol{\theta}$, and is a (rudimentary) structure providing a feedback $\boldsymbol{\pi}^s$ as described in Section II-C. In practice, (76) is equivalent to a tube-based MPC.

C. Simulation setup & results

The simulations proposed here use the same setup as the companion paper [10] treating the stochastic policy gradient case, so as to make comparisons straightforward. The experimental parameters are summarized in Tab. I and:

$$\mathbf{x}_{k+1} = A_{\text{real}}\mathbf{x}_k + B_{\text{real}}\mathbf{u}_k + \mathbf{n}, \quad (77)$$

where the process noise \mathbf{n} is selected Normal centred, and clipped to a ball. The real system was selected as:

$$A_{\text{real}} = \kappa \begin{bmatrix} \cos \beta & \sin \beta \\ \sin \beta & \cos \beta \end{bmatrix}, B_{\text{real}} = \begin{bmatrix} 1.1 & 0 \\ 0 & 0.9 \end{bmatrix}. \quad (78)$$

The real process noise \mathbf{n} is chosen normal centred of covariance $\frac{1}{3}10^{-2}I$, and restricted to a ball of radius $\frac{1}{2}10^{-2}$. The initial nominal MPC model is chosen as:

$$A_0 = \begin{bmatrix} \cos \hat{\beta} & \sin \hat{\beta} \\ \sin \hat{\beta} & \cos \hat{\beta} \end{bmatrix}, B_0 = \begin{bmatrix} 1 & 0 \\ 0 & 1 \end{bmatrix}, \mathbf{b}_0 = \begin{bmatrix} 0 \\ 0 \end{bmatrix}. \quad (79)$$

and $N_M = 4$ with:

$$\mathbf{W}^1 = \frac{1}{10} \begin{bmatrix} -1 \\ -1 \end{bmatrix}, \quad \mathbf{W}^2 = \frac{1}{10} \begin{bmatrix} +1 \\ -1 \end{bmatrix} \quad (80a)$$

$$\mathbf{W}^3 = \frac{1}{10} \begin{bmatrix} +1 \\ +1 \end{bmatrix}, \quad \mathbf{W}^4 = \frac{1}{10} \begin{bmatrix} -1 \\ +1 \end{bmatrix}. \quad (80b)$$

TABLE I: Simulation parameters

Parameter	Value	Description
γ	0.99	Discount factor
Σ	I	Exploration shape
σ	10^{-3}	Exploration covariance
τ	10^{-2}	Relaxation parameter
β	22°	Real system parameter
$\hat{\beta}$	20°	Model parameter
N_t	20	Sample length
S	30	Number of sample per batch
N	10	MPC prediction horizon

The baseline stage cost is selected as:

$$L = \frac{1}{20} \|\mathbf{x} - \mathbf{x}_{\text{ref}}\|^2 + \frac{1}{2} \|\mathbf{u} - \mathbf{u}_{\text{ref}}\|^2 \quad (81)$$

and serves as the baseline performance criterion to evaluate the closed-loop performance of the MPC scheme.

We considered two cases, using deterministic initial conditions $\mathbf{s}_0 = [\cos 60^\circ \quad \sin 60^\circ]^\top$. Both cases consider the parameters $\theta = \{\bar{\mathbf{x}}, \bar{\mathbf{u}}, A_0, B_0, \mathbf{b}_0, K, \mathbf{W}\}$. The first case considers a stable real system with $\kappa = 0.95$, the second case considers an unstable real system with $\kappa = 1.05$. In both cases, the target reference $\bar{\mathbf{x}}$ was provided, together with the input reference $\bar{\mathbf{u}}$ delivering a steady-state for the nominal MPC model. The feedback matrix K was chosen as the LQR controller associated to the MPC nominal model. Table I reports the algorithmic parameters. Case 1 used a step size $\alpha = 0.05$, the second case used a step size $\alpha = 0.01$. The results for the first case are reported in Figures 4-8. One can observe in Fig. 4 that the closed-loop performance is improving over the RL steps. Fig. 5 shows that the improvement takes place via driving the closed-loop trajectories of the real

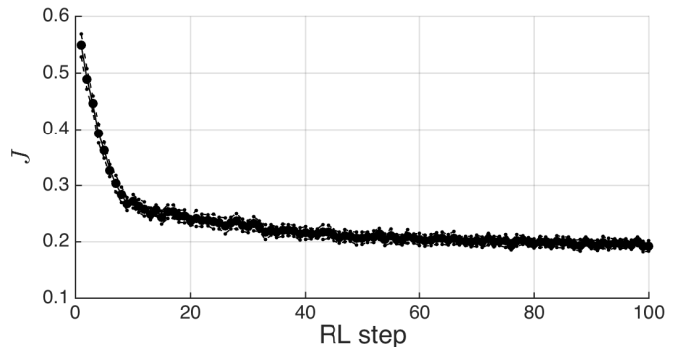


Fig. 4: Case 1. Evolution of the closed-loop performance J over the RL steps. The solid line represents the estimation of J based on the samples obtained in the batch. The dashed line represent the standard deviation due to the stochasticity of the system dynamics and policy disturbances.

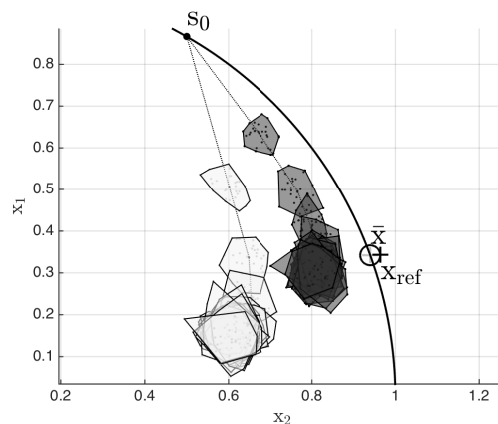


Fig. 5: Case 1. Closed-loop system trajectories. The initial conditions \mathbf{s}_0 are reported, as well as the target state reference \mathbf{x}_{ref} (circle), and the MPC reference $\bar{\mathbf{x}}$ at the first RL step and at the last one (grey and black + symbol respectively). The trajectories at the first and last RL steps are reported as the light and dark grey polytopes. The solid black curve represents the state constraint $\|\mathbf{x}\|^2 \leq 1$.

system closer to the reference, without jeopardising the system safety. Fig. 6 shows how the RL algorithm uses the MPC nominal model to improve the closed-loop performance. One can readily see from Fig. 6 that RL is not simply performing system identification, as the nominal MPC model developed by the RL algorithm does not tend to the real system dynamics. Fig. 7 shows how the RL algorithm reshapes the dispersion set. The upper-left corner of the set is the most critical in terms of performance, as it activates the state constraint $\|\mathbf{x}\|^2 \leq 1$, and is moved inward to gain performance. The constrained RL step (71) ensures that the RL algorithm cannot jeopardize the system safety. In Fig. 8, one can see that the RL algorithm does not use much the degrees of freedom provided by adapting the MPC feedback matrix K .

The results for case 2 are reported in Figures 9-13. Similar comments hold for case 2 as for case 1. The instability of the real system does not challenge the proposed algorithm, even though a smaller step size σ had to be used as the RL algorithm appears to more sensitive to noise.

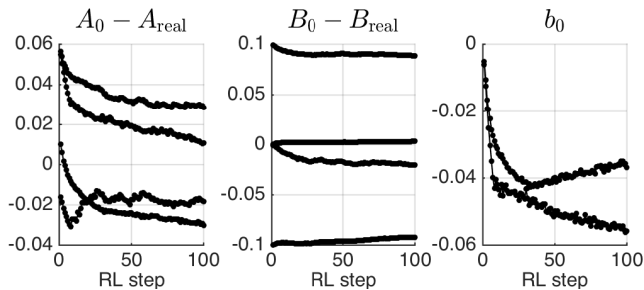


Fig. 6: Case 1. Evolution of the nominal MPC model over the RL steps. We report here the difference between the nominal model used in the MPC scheme and the real system.

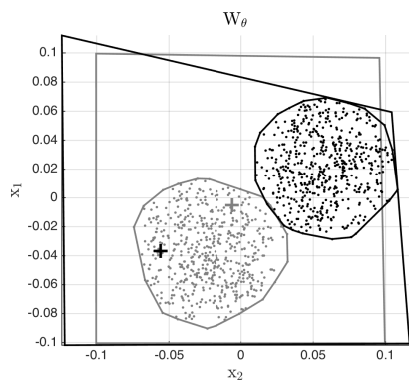


Fig. 7: Case 1. Evolution of the MPC model biases $\mathbf{W}^{1, \dots, M}$ over the RL steps. The light grey polytope depicts the biases at the first RL step, and the points show $\mathbf{s}_{k+1} - \mathbf{F}_0(\mathbf{s}_k, \mathbf{a}_k, \boldsymbol{\theta})$ for all the samples of the first batch of data. The + symbol reports the initial nominal model offset \mathbf{b}_0 . The cloud of point is inside the grey quadrilateral thanks to the constrained RL step (71). The same objects are represented in black for the last step of the learning process.

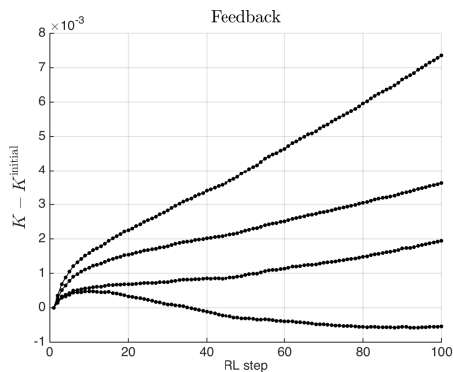


Fig. 8: Case 1. Evolution of the MPC feedback matrix K from its initial value. The feedback is only marginally adjusted by the RL algorithm. After 100 RL steps, the adaptation of the feedback gain K has not yet reached its steady-state value.

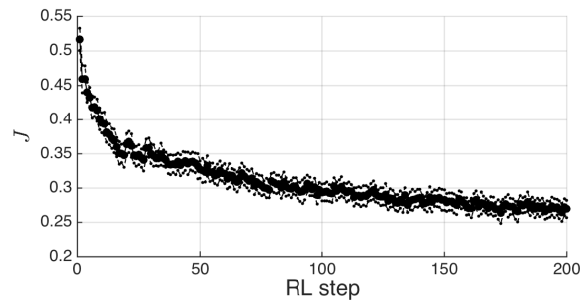


Fig. 9: Case 2, similar to Fig. 4.

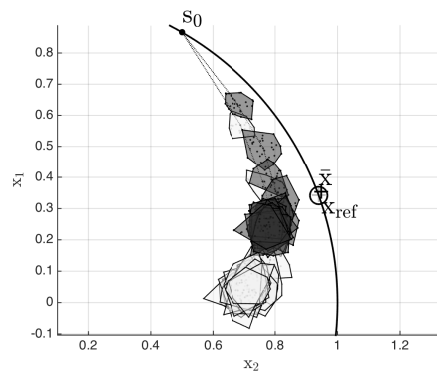


Fig. 10: Case 2, similar to Fig. 5

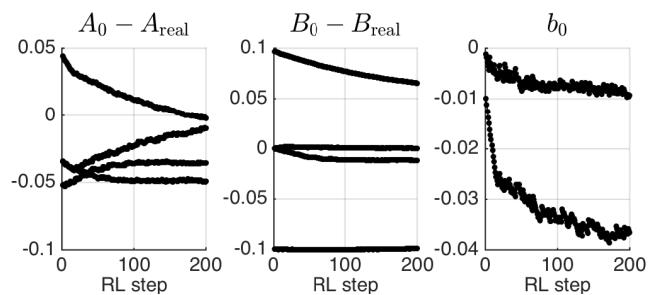


Fig. 11: Case 2, similar to 6.

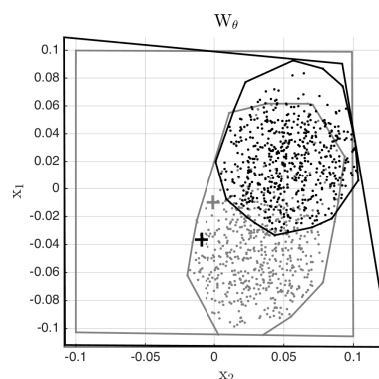


Fig. 12: Case 2, similar to Fig. 7.

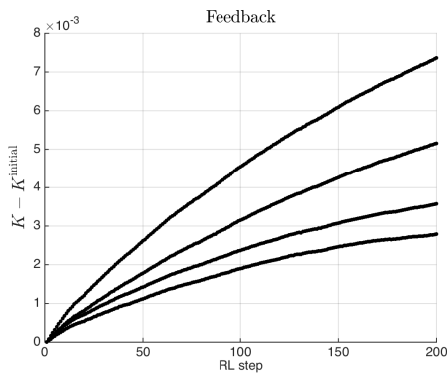


Fig. 13: Case 2, similar to Fig. 8.

VIII. CONCLUSION

This paper proposed a technique to deploy deterministic policy gradient methods using a constrained parametric optimization problem as a support for the optimal policy approximation. This approach allows one to impose strict safety constraints on the resulting policy. In particular, robust Nonlinear Model Predictive Control, where safety requirements can be imposed explicitly, can be selected as a parametric optimization problem. Imposing restrictions on the policy approximation creates some technical challenges when generating the exploration required to form the policy gradient. Computationally inexpensive methods are proposed here to tackle these challenges, using interior-point techniques when solving the parametric optimization problem. The specific case of robust Model Predictive Control, where the prediction model is linear, is further developed, and a methodology to impose safety requirements throughout the learning process is proposed. The proposed techniques are illustrated in simple simulations, showing their behavior. This paper has a companion paper [10] investigating the stochastic policy gradient approach in the same context as in this paper. In the simulations performed here, the stochastic policy gradient approach of [10] appears to be computationally more expensive than the approach proposed here.

REFERENCES AND NOTES

- [1] Pieter Abbeel, Adam Coates, Morgan Quigley, and Andrew Y. Ng. An application of reinforcement learning to aerobatic helicopter flight. In *Advances in Neural Information Processing Systems 19*, page 2007. MIT Press, 2007.
- [2] D. Bernardini and A. Bemporad. Scenario-based model predictive control of stochastic constrained linear systems. In *Proceedings of the 48th IEEE Conference on Decision and Control (CDC) held jointly with 2009 28th Chinese Control Conference*, pages 6333–6338, Dec 2009.
- [3] D. Bertsekas. *Dynamic Programming and Optimal Control*, volume 2. Athena Scientific, 3rd edition, 2007.
- [4] D.P. Bertsekas. *Dynamic Programming and Optimal Control*, volume 1 and 2. Athena Scientific, Belmont, MA, 1995.
- [5] D.P. Bertsekas and I.B. Rhodes. Recursive state estimation for a set-membership description of uncertainty. *IEEE Transactions on Automatic Control*, 16:117–128, 1971.
- [6] D.P. Bertsekas and S.E. Shreve. *Stochastic Optimal Control: The Discrete Time Case*. Athena Scientific, Belmont, MA, 1996.
- [7] Lorenz T. Biegler. *Nonlinear Programming*. MOS-SIAM Series on Optimization. SIAM, 2010.

- [8] T. Ensslin. *Information Field Theory*. arXiv:1301.2556 [astro-ph.IM], 2013.
- [9] S. Gros and M. Zanon. Data-Driven Economic NMPC using Reinforcement Learning. *IEEE Transactions on Automatic Control*, 2018. (in press).
- [10] S. Gros and M. Zanon. Towards Safe Reinforcement Learning Using NMPC and Policy Gradients - Stochastic case (Part I). *IEEE Transactions on Automatic Control*, 2019. (submitted).
- [11] Oehlert G.W. A note on the delta method. *The American Statistician*, 46(1), 1992.
- [12] J. Fernandez J. Garcia. A comprehensive survey on safe reinforcement learning. *Journal of Machine Learning Research*, 16:1437–1480, 2013.
- [13] I. Kolmanovsky and E.G. Gilbert. Theory and computation of disturbance invariant sets for discrete-time linear systems. *Math. Probl. Eng.*, 4(4):317–367, 1998.
- [14] David Q. Mayne. Model predictive control: Recent developments and future promise. *Automatica*, 50(12):2967 – 2986, 2014.
- [15] J. Nocedal and S.J. Wright. *Numerical Optimization*. Springer Series in Operations Research and Financial Engineering. Springer, 2 edition, 2006.
- [16] P. O. M. Scolaert and D. Q. Mayne. Min-max feedback model predictive control for constrained linear systems. *IEEE Transactions on Automatic Control*, 43:1136–1142, 1998.
- [17] David Silver, Guy Lever, Nicolas Heess, Thomas Degris, Daan Wierstra, and Martin Riedmiller. Deterministic policy gradient algorithms. In *Proceedings of the 31st International Conference on Machine Learning, ICML'14*, pages I–387–I–395, 2014.
- [18] Richard S. Sutton, David McAllester, Satinder Singh, and Yishay Mansour. Policy gradient methods for reinforcement learning with function approximation. In *Proceedings of the 12th International Conference on Neural Information Processing Systems, NIPS'99*, pages 1057–1063, Cambridge, MA, USA, 1999. MIT Press.
- [19] Shouyi Wang, Wanpracha Chaovaitwongse, and Robert Babuska. Machine learning algorithms in bipedal robot control. *Trans. Sys. Man Cyber Part C*, 42(5):728–743, September 2012.
- [20] M. Zanon and Gros. Safe Reinforcement Learning Using Robust MPC. In *Transaction on Automatic Control, Archivr*, 2019. (submitted).



Sébastien Gros received his Ph.D degree from EPFL, Switzerland, in 2007. After a journey by bicycle from Switzerland to the Everest base camp in full autonomy, he joined a R&D group hosted at Strathclyde University focusing on wind turbine control. In 2011, he joined the university of KU Leuven, where his main research focus was on optimal control and fast NMPC for complex mechanical systems. He joined the Department of Signals and Systems at Chalmers University of Technology, Göteborg in 2013, where he became associate Prof.

in 2017. He is now full Prof. at NTNU, Norway and guest Prof. at Chalmers. His main research interests include numerical methods, real-time optimal control, reinforcement learning, and the optimal control of energy-related applications.



Mario Zanon received the Master's degree in Mechatronics from the University of Trento, and the Diplôme d'Ingénieur from the Ecole Centrale Paris, in 2010. After research stays at the KU Leuven, University of Bayreuth, Chalmers University, and the University of Freiburg he received the Ph.D. degree in Electrical Engineering from the KU Leuven in November 2015. He held a Post-Doc researcher position at Chalmers University until the end of 2017 and is now Assistant Professor at the IMT School for Advanced Studies Lucca. His research interests

include numerical methods for optimization, economic MPC, optimal control and estimation of nonlinear dynamic systems, in particular for aerospace and automotive applications.